processes

MDPI

Article

A Hybrid Modeling Framework for Membrane Separation Processes: Application to Lithium-Ion Recovery from Batteries

Maria João Regufe, Vinicius V. Santana *, Alexandre F. P. Ferreira, Ana M. Ribeiro, José M. Loureiro and Idelfonso B. R. Nogueira *

Laboratory of Separation and Reaction Engineering, Associate Laboratory LSRE/LCM, Department of Chemical Engineering, Faculty of Engineering, University of Porto, 4200-465 Porto, Portugal; mjregufe@fe.up.pt (M.J.R.); aferreira@fe.up.pt (A.F.P.F.); apeixoto@fe.up.pt (A.M.R.); loureiro@fe.up.pt (J.M.L.)

* Correspondence: up201700649@fe.up.pt (V.V.S.); idelfonso@fe.up.pt (I.B.R.N.)

Abstract: This study proposed a hybrid modeling framework for membrane separation processes where lithium from batteries is recovered. This is a pertinent problem nowadays as lithium batteries are popularized in hybrid and electric vehicles. The hybrid model is based on an artificial intelligence (AI) structure to model the mass transfer resistance of several experimental separations found in the literature. It is also based on a phenomenological model to represent the transient system regime. An optimization framework was designed to perform the AI model training and simultaneously solve the Ordinary Differential Equation (ODE) system representing the phenomenological model. The results demonstrate that the hybrid model can better represent the experimental validation sets than the phenomenological model alone. This strategy opens doors for further investigations of this system.

Keywords: hybrid modeling; membrane separation; artificial neural network; lithium recovery

Citation: Regufe, M.J.; Santana, V.V.; Ferreira, A.F.P.; Ribeiro, A.M.; Loureiro, J.M.; Nogueira, I.B.R. A Hybrid Modeling Framework for Membrane Separation Processes: Application to Lithium-Ion Recovery from Batteries. *Processes* **2021**, *9*, 1939. https://doi.org/10.3390/pr9111939

Academic Editor: Xu Ji

Received: 30 September 2021
Accepted: 27 October 2021
Published: 29 October 2021

1. Introduction

Phenomenological modeling is an essential step for systems design, development, and optimization. Usually, phenomenological modeling is done by applying conservation laws, capable of representing the known phenomenology through one or a system of differential equations. Though consolidated and reliable, this approach requires more significant computational effort to provide the results. The more complex the system is, the more complex the model itself becomes. On the other hand, the modeling of first principles is usually associated with system parameters, such as mass transfer coefficient, reaction rate, etc. These parameters are generally embedded into a constant that needs to be estimated through experimental data. Thus, the way these parameters are added in the conservation laws is usually associated with simplifications that allow the model to be identifiable. This is a limiting factor that will be reflected in the model precision and reliability.

Empirical modeling is presented as an alternative to phenomenological modeling; it is a data-oriented strategy that extracts the system information and stores it into the model structure. Data-driven empirical modeling has been explored in chemical engineering to solve several problems in this field [1–4]. This strategy efficiently identifies reliable models with low computational effort and can be easily applied in online applications. On the other hand, empirical modeling requires a significant amount of data to be identified due to its limited extrapolation capacity.

The advances in both fields, phenomenological and empirical modeling, led to hybrid models, namely, hybrid models based on artificial intelligence [4–6]. This strategy leverages both strategies' advantages to build a more complex and reliable model without increasing the associated computational effort. In Nagrath et al. (2004) [7], a hybrid modeling framework for chromatographic processes optimization is presented. The authors highlight the ability of the proposed strategy to explore several different design scenarios

without additional computational effort. Still, in the chromatographic separation field, Narayanan et al. (2021) [4] presented a study regarding a phenomenological model hybridization level. The authors point to the gains in prediction accuracy and extrapolation ability as the main advantages of this strategy.

Furthermore, the referred work indicates that these solutions are more likely to be implemented in practical applications. Even though the potential of hybrid modeling is emphasized in the literature, its application to address chemical engineering problems is still shy. For instance, in the membrane separation field, it would have the potential to address issues related to identifying a proper strategy to model the system mass transfer resistances. Membrane separation is composed of a series of elements that promote a driving force between the membrane sides, thereby promoting separation. These elements are translated into mass transfer resistance coefficients that should be estimated to obtain a phenomenological system model. As an alternative, a global mass transfer coefficient can be defined to simplify the model and the system identification. In this scenario, the hybrid modeling approach presents the potential to address this problem to provide more versatility and flexibility to the membrane models.

Hence, this study proposed a hybrid modeling framework for membrane separation processes. The presented case study was the recovery of lithium from batteries, which is a pertinent case in the scenario nowadays where lithium batteries are popularized in hybrid and electric vehicles. The proposed framework used artificial intelligence (AI) structures to model the mass transfer resistance of several experimental separations found in the literature. The AI models were incorporated into the phenomenological membrane model. An optimization strategy trained the AI model and simultaneously solved the Ordinary Differential Equation (ODE) that represents the phenomenological model.

Case Study: Lithium-Ion Recovery from Batteries

Solvent extraction, membrane separation, adsorption, and electrochemical methods are the most common techniques used for lithium separation from spent lithium-ion batteries (LIBs). Liquid membrane techniques, mainly supported liquid membranes (SLMs), have been increasingly studied for treating and purifying solutions in hydrometallurgical industries [8–11]. SLM can be designed in several configurations: flat-sheet supported liquid membranes (FSSLM), and hollow-fiber supported liquid membranes (HFSLM).

The mass flux of a species is defined as the amount of matter passing through an area unit during a time unit [12]. This flux is dependent on a variety of factors, such as choice and concentrations of carrier and solvents, choice and type of membrane support, and volumes of aqueous phases. To estimate or represent the experimental data of separations, several parameters must be measured experimentally, such as permeabilities and mass transfer coefficients. However, in addition to the costs related to the experimental work, if experimental data are unavailable or challenging to obtain, it is essential to have a preview or an estimation for the solute transference somehow. In this context, Regufe et al. (2021) [13] presented a complete model to be applied in flat-sheet supported liquid membranes to estimate the behavior of solute concentration in feed and receiving phases during operation. To assess the process dynamic behavior, a phenomenological model, which can be complex, was used, and its simulation could require great computational time and effort. For the industry, the simplification of this model can be helpful to predict mass transfer in a simple way, which was proposed again in the work reported by Regufe et al. (2021) [13]. The simplified model proposed the estimation of the global ionic mass transfer resistance needing only a few experiments. However, the prediction needs to use the experimental data of the feed and receiving phases. This assessment in the real-time process is challenging, which is a barrier to using a phenomenological model. Therefore, it is necessary to find alternative models that can provide accurate information about the process dynamics in real-time.

The use of lithium-ion batteries in several applications, namely, for the operation of hybrid and electric vehicles, has increased exponentially in recent years [14]. In this

way, lithium consumption has grown. The extraction of lithium from brines and hard rock deposits is the main pathway to face the increasing demand. Sun et al. (2019) [15] presented a complete overview of lithium extraction and separation from salt lake brine. The authors of the referred work pointed out the increasing demand for lithium due to the rapid development of applications that need this resource, such as lithium batteries. They also presented a series of alternative methods for lithium separation and recovery, including membranes separation. Zheng et al. (2020) [16] offered a review of the importance of lithium as a functional chemical in batteries. The authors analyzed the structural, electrokinetic, and electrochemical aspects to improve the batteries' efficiency.

Lithium producers are limited, operating essentially in the USA, Canada, Russia, Chile, Argentina, Australia, and China [17]. The need for lithium recovery is increasing worldwide. The quantity of this ion present in batteries is about 5 to 7%, being a potential source for recovery of lithium-ion [18], much higher than the content in natural ores. The recycling of spent LIBs has considerable prospects. It is environmentally friendly, so it is imperative to establish a sound recycling system, implying an investment in research related to recycling technologies. However, secondary lithium recycling sources are scarce in the hydrometallurgical recycling of lithium from spent lithium-ion batteries until now. In addition to the environmental aspects, the requirements of purity for specific applications, the production, and recovery costs are essential aspects to be considered in the decision. Another critical aspect in the decision is the presence of other constituents in the batteries, such as cobalt, nickel, and other metals (copper, aluminum, iron, chromium, and others). The recovery of other metals, namely, cobalt, can be the priority for studies due to its value and importance to lithium-battery chemistries. The global demand for cobalt will increase 60% above 2017 levels by 2025, with batteries projected to make up more than half of that use [19]. Thus, the demand for separation, purification, and recovery methods is currently receiving great attention.

Overall, the literature demonstrates the increasing necessity for ways to efficiently recover lithium due to the popularization of the employment of lithium to store energy. Hence, one of the primary sources of lithium will soon be its recovery from batteries. Even though lithium has a prominent role in energy storage, other metals start to present potential in these applications, such as Al and Zn, as argued by Zheng et al. (2021a) [20] and Zheng et al. (2021b) [16]. Therefore, while it is essential to study lithium recovery, it is also necessary to develop strategies that address other metals' recovery or separation. In this context, the methodology proposed in this study covered not only lithium separation but metals separation in general.

In this context, the present study used a flat-sheet supported liquid membrane (FSSLM) for lithium recovery as a case study. FSSLM is the most usual and most straightforward type of liquid membrane supported in microporous solids. The membrane was positioned between two sections: a section where the solution was fed and another for the stripping solution; these sections were stirred by mechanical agitation. This unit is depicted in Figure 1, and its main advantage was the simple assembling. On the other hand, it presented a low surface area as the main drawback.

In the next section, the proposed hybrid ordinary differential equation/artificial neural network (ODE-ANN) model is presented. This novel strategy is compared to a phenomenological model of this system to understand better the methodology proposed here. Furthermore, the objective function of the system identification step is presented together with the parameters estimation strategy.

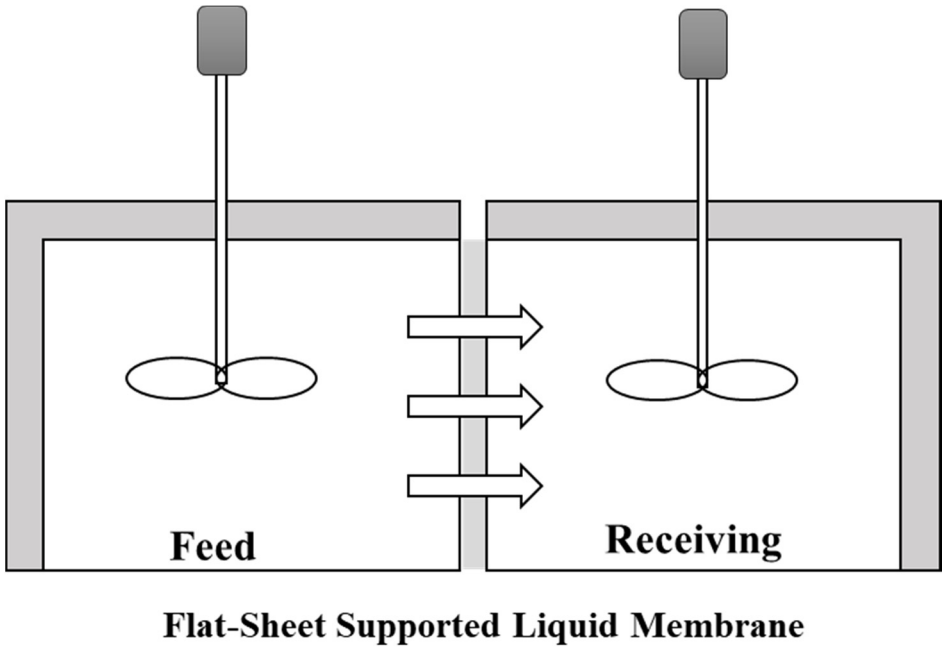

Figure 1. Schematic representation of an FSSLM.

2. Materials and Methods

2.1. Hybrid Model

The phenomenology involved in a liquid membrane separation comprises the aqueous feed phase, the organic phase (membrane), and the aqueous receiving phase. The existing literature provides first-principle models representing the transport mechanism through the supported liquid membrane containing different carriers. Regufe et al. (2021) [13] presented a phenomenological model for the present case study. In the referred work, the authors developed a simplified strategy to identify phenomenological models for membrane separation using few experimental data for model validation [13]. The Regufe et al. method identified two time constants, one for the receiving phase and another for the feed phase, to improve the model accuracy. This strategy was demonstrated to have accuracy close to more-detailed phenomenological modeling strategies. Therefore, the phenomenological model proposed in Regufe's et al. that considers an overall mass transfer coefficient was here used as a base. A schematic representation of the membrane transport profile is depicted in Figure 2. This transport phenomenon was composed of a solute, *S*, that reacts with the carrier, *E*, at the feed–membrane interface, forming the complex species, *C*. The complex species diffuses through the liquid membrane until it reaches the membrane–strip interface, where it reacts with the stripping solution. Then, the concentration gradient will promote a driving force that will conduct this solute in the strip solution diffusing towards the bulk strip solution.

This system, extraction of a metal ion by FSSLM, is portrayed by the following equilibrium, which is valid at both interfaces (feed/membrane and membrane/receiving):

$$S + \alpha \cdot E \overset{K_e}{\leftrightarrow} C + \beta \cdot X \quad (1)$$

with *S* as the solute, *E* as the carrier at the membrane interfaces, *C* as the complex species, *X* as the component in the carrier exchanged with *S* (if the solute is an ion, then *X* is denominated as counter-ion), and α and β as the stoichiometric coefficients.

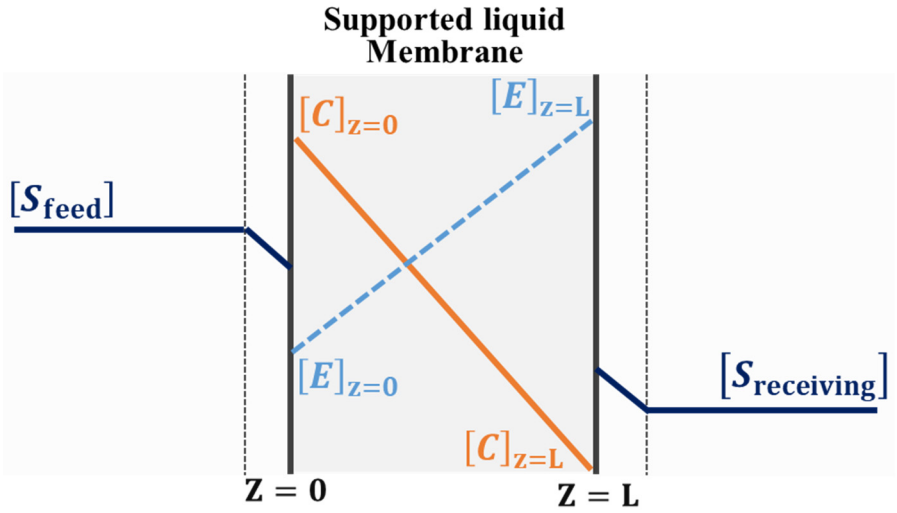

Figure 2. Schematic representation of the membrane transport profile: solute (S), metal-carrier complex (C), and carrier (E) (based on Patil et al. [21]).

Assuming ideal behavior, the system dynamic behavior can be described, as proposed by Regufe et al. (2021) [13], as:

$$-\frac{dS_F}{dt} = \varphi_f\left(V_f, A, S_{f,0}\right)\left(S_f - S_{f,i}\right) \quad (2)$$

where φ_f is an empirical model that describes the mass transfer coefficient in the feed–membrane interface, S_f and $S_{f,i}$ are, respectively, the solute/metal concentrations at the feed phase and the feed–membrane interface, $S_{f,0}$ is its corresponding initial concentration, V_f is the feed phase volume, and A is the effective interfacial area. It is essential to highlight that, differently from a solely phenomenological model, the proposed strategy uses an empirical model (artificial neural network) to portray the film-diffusion transport mechanism. Usually, this phenomenon is described by a single parameter, which was also implemented here to provide a comparison source to the proposed approach.

To estimate $S_r{}^*$, Equation (3) was used:

$$S_r{}^* = S_r\left(\frac{X_f}{X_r}\right)^{\beta} \quad (3)$$

where X_r represents the component in the carrier exchanged with S_r, X_f represents the component in the carrier exchanged with S_f (when the solute is an ion, X is denominated as counter-ion), and β represents the stoichiometric coefficient.

The accumulation in the membrane phase is neglected and the conservation in both S and X species was imposed; Equations (4) and (5) result from this:

$$V_f\left(S_{f,0} - S_f\right) = V_r(S_r - S_{r,0}) \quad (4)$$

$$V_f\left(X_f - X_{f,0}\right) = V_r(X_{r,0} - X_r) \quad (5)$$

The stoichiometric exchange at the feed/membrane interface gave Equation (6):

$$\beta\left(S_{f,0} - S_f\right) = \left(X_f - X_{f,0}\right) \quad (6)$$

The mass balance for the receiving phase was computed by:

$$\frac{dS_r}{dt} = \varphi_r(V_r, A, S_{r,0})(S_{r,i} - S_r) \quad (7)$$

where V_r is the receiving phase volume, and S_r, $S_{r,0}$, and $S_{r,i}$ represent the solute concentration at the receiving phase and the membrane–receiving interface. As in Equation (2), the concentration in the receiving phase was conditioned by the stagnant film in the interphase; at this point, the film diffusion was the transport mechanism. As previously mentioned, the present work leveraged the potential of the artificial neural network (ANN) model to precisely model this phenomenon, building a hybrid model.

Then, the conservation of counter-ions in the receiving phase was given by:

$$X_r = X_{r,0} - \beta(S_r - S_{r,0}) \tag{8}$$

where X_r is the component in the carrier exchanged with S_r.

The model was implemented in Python, and it was validated using experimental data from the literature, as will be detailed in the following sections.

2.2. Data Collection

FSSLM has gained attention in lithium recovery from spent lithium-ion batteries. In this context, the development of models to represent the transport mechanism through the supported liquid membranes is essential to reduce experimental test-work and, consequently, decrease costs. Besides lithium, it is crucial to study other metal ions' transport behavior or solutes in wastewater treatment. In this context, experimental data of separation and extraction of metal ions from aqueous phases using FSSLM were collected to train and validate the models. The details of each data set used are presented in Table 1. Please note that each training set means an identification procedure for a specific ion. Thus, the ANNs represent the mass transfer for a particular ion given its inputs, as presented in Equations (2) and (7).

Table 1. Details for the experimental data collected in the literature and used to train and validate the hybrid model.

	Reference	Characteristics
Training and Validation sets I	[22]	Extraction of two heavy metals, lead(II) and cadmium(II) Feed and receiving phases: 250 cm^3 Area: 8.0 cm^2 Carrier-solvent: sodium salt of Di-2-ethylhexylphosphoric acid (D2EHPA)
Training and Validation sets II	[23–25]	Extraction of lithium Feed and receiving phases: 250 cm^3 Area: 8.0 cm^2 Carrier-solvent: Cyanex272
Training and Validation sets III	[26]	Extraction of cobalt and nickel Feed and receiving phases: 250 cm^3 Area: 17.8 cm^2 Carrier-solvent: tri(hexyl)tetradecyl phosphonium chloride
Training and Validation sets IV	[25]	Transport of Ge(IV) Feed and receiving phases: 60 cm^3 Area: 4.5 cm^2 Carrier-solvent: Alamine 336

2.3. Hybrid Model Identification

With the hybrid model proposed, the next step was to address the issues related to the model identification. As it is a structure composed of phenomenological and empirical models, its identification should comprise its peculiarities. Regarding the phenomenological model, it is a system of ODE equations, which are solved by a conventional Runge–Kutta algorithm. However, the phenomenological part depends on the empirical part, which

requires an identification step. Therefore, a framework for this model identification needed to be established. The framework proposed here was based on the work of Narayana et al. (2021). A scheme of this framework is provided in Figure 3 depicting an overview of the employed strategy. It consists of an initial step of initialization of the empirical model parameters ($w_{1,1}$ to $w_{1,n}$, $w_{2,1}$ to $w_{2,n}$, $w_{3,1}$ to $w_{3,n}$, $w_{2,2}$ to $w_{2,n}$, $b_{1,1}$ to $b_{1,n}$, and $b_{2,2}$ to $b_{2,n}$). These parameters needed to be estimated based on the experimental data collected in the literature. The solution of the empirical model provided the mass transfer information to the phenomenological model, which, in turn, was solved by the numerical method. Thus, a predicted value of system concentrations was given, which was used to compute the parameter-estimation objective function. The particle swarm optimizer calculated the new set of parameters values, sending it back to the neural network. This procedure was repeated until the objective function was minimized and the required model precision was achieved. Each one of these layers is described in the following items of this section.

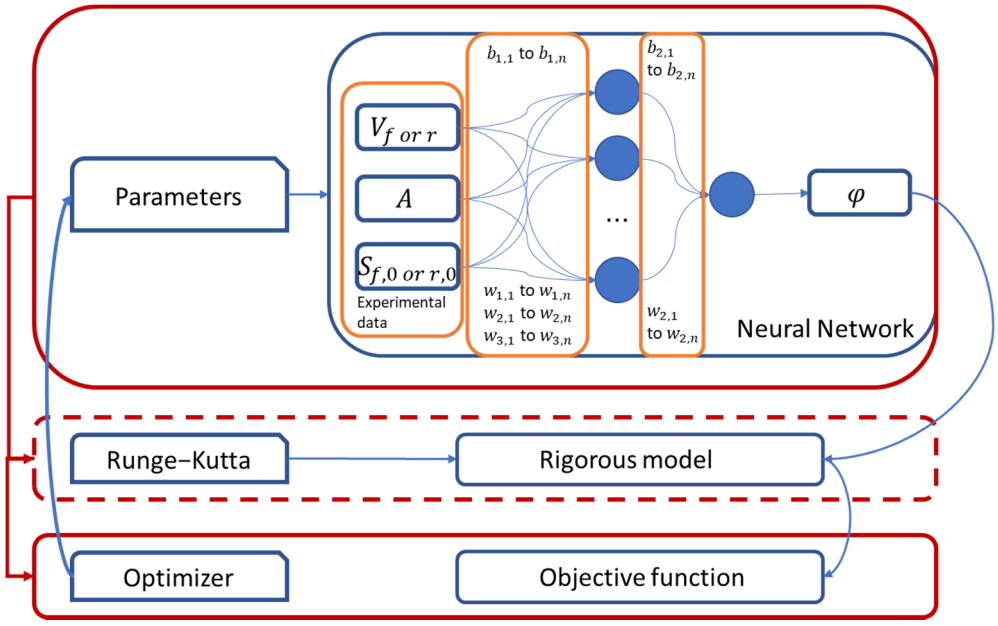

Figure 3. Schematic representation of the proposed framework.

2.4. Parameter-Estimation Problem

As shown in Figure 3, the last layer of the proposed identification framework is parameter estimation. Therefore, an objective function was designed to address the proposed problem. The objective function here adopted was based on the difference between the predicted concentration and the experimental concentration. However, it is essential to note that the ANN models, whose parameters were estimated, do not predict the concentrations. Instead, they predict the mass transfer effects in the system, as previously described. In this way, the solution of the parameter-estimation problems required the complete resolution of the hybrid model. This strategy goes against the usual approach in ANN model identification, where the ANN models are identified independently and are meant to predict the main property directly. Therefore, this step needed to be performed simultaneously with the solution of the complete hybrid model. Hence, the objective function that needed to be solved to proceed with the parameter estimation was defined as a least-square problem, as:

$$\min_{\lambda} F_{obj} = \sum_{j=1}^{NS} \sum_{i=1}^{NE} \left[(S_r - S_r^e)^2 + \left(S_f - S_f^e \right)^2 \right]$$

$$\text{s.t. :} \quad S_f = \mathbf{f}\left(\varphi_f \left(V_f A \; S_{f,0} \right) \right) \tag{9}$$

$$S_R = \mathbf{f}(\varphi_r (V_r A \; S_{r,0}))$$

where NE is the total number of experimental points in the experimental set, and NS is the number of experimental sets. S_r^e and S_f^e represent the experimental solute concentrations at the receiving and feed phases, and $\boldsymbol{\lambda}$ is the set of decision variables of the problem, in this case, the matrix of ANN's parameters to be estimated.

3. Results

Finally, the framework presented here could be applied in identifying and validating the hybrid model for the FSSLM process. Therefore, the optimization problem described in Section 3 needed to be solved. It was solved using a Constrained Sliding Particle Swarm optimization (CSPSO) proposed by Rebello et al. (2021) [27] with 400 particles and 400 iterations. The CSPSO was applied due to its coping with multimodal problems, as in the present case. Therefore, following this trial-and-error strategy, an optimal number of neurons equal to 20 in one hidden layer was identified, activated by hyperbolic tangent functions.

The hybrid modeling strategy proposed here was applied to model lithium recovery in an FSSLM process. The case study evaluated for lithium separation was a highly selective membrane for lithium cations, as previously reported in the literature. In Zante et al. (2020) [24], the lithium transport across this supported liquid membrane was reported. The referred work demonstrates that lithium cations are selectively separated from aqueous solutions containing sodium, cobalt, and nickel ions in this membrane separation. This provides evidence for the potential of this process in the recovery of lithium from battery solution. The experimental data used to validate the proposed strategy were obtained from Zante et al. (2019) [25], presenting a liquid membrane with very high selectivity for the separation of lithium from sodium. These experimental data were obtained for a feed of LiCl (0.1 mmol/L), pH = 12, and a supported liquid membrane HFDOD (0.2 mol/L) and TOPO (0.1 mol/L).

The models were identified using the literature data, and validation was conducted against another independent literature data set. Figure 4 presents the models' validation with the sole phenomenological model prediction obtained from Regufe et al. (2021) [13] to compare the proposed approach. The phenomenological model used two different time constants, one for the feed and another for the receiving, as presented in Regufe's work, to keep a fair comparison between the strategies.

Furthermore, the parity graphics are provided as an interpolation test. Figure 4 presents the first experimental set of validation. These results demonstrate the lithium was diffusively transported through the membrane. The experiment shown in Figure 4 depicts a fast decrease in lithium concentration until 50% in the feed side, accompanied by a rapid increase in lithium in the receiving side, also until 50%. After that, it took about 1200 minutes until the almost complete removal of lithium from the feed stream. It is an interesting case because it portrays the process dynamics within a full range of concentration variations. The lithium concentration ranged from approximately 100% to 0% on both sides of the initial feed concentration. This exemplifies a wide range of concentrations where the model can efficiently predict the system behavior. As it is possible to see in Figure 4, the hybrid (H-model) approach could precisely predict the model system dynamics behavior. In contrast, the phenomenological model (R-model) presents limitations with portraying the total system dynamics.

Still, in Figure 4, it is possible to analyze the model residuals in the parity graphics, which display the hybrid model prediction versus the experimental data and the phenomenological model prediction versus the experimental data. The plots display point density along the diagonal line. It can be seen that the predictions from the hybrid model are randomly distributed around the diagonal line across the whole range of values. This is evidence that the residuals were random. Therefore, the model was satisfactorily identified. In contrast, the phenomenological model presents a nonrandom pattern within some regions. These points correspond to the transient regime of the process, pointed out to be a limitation in the phenomenological model.

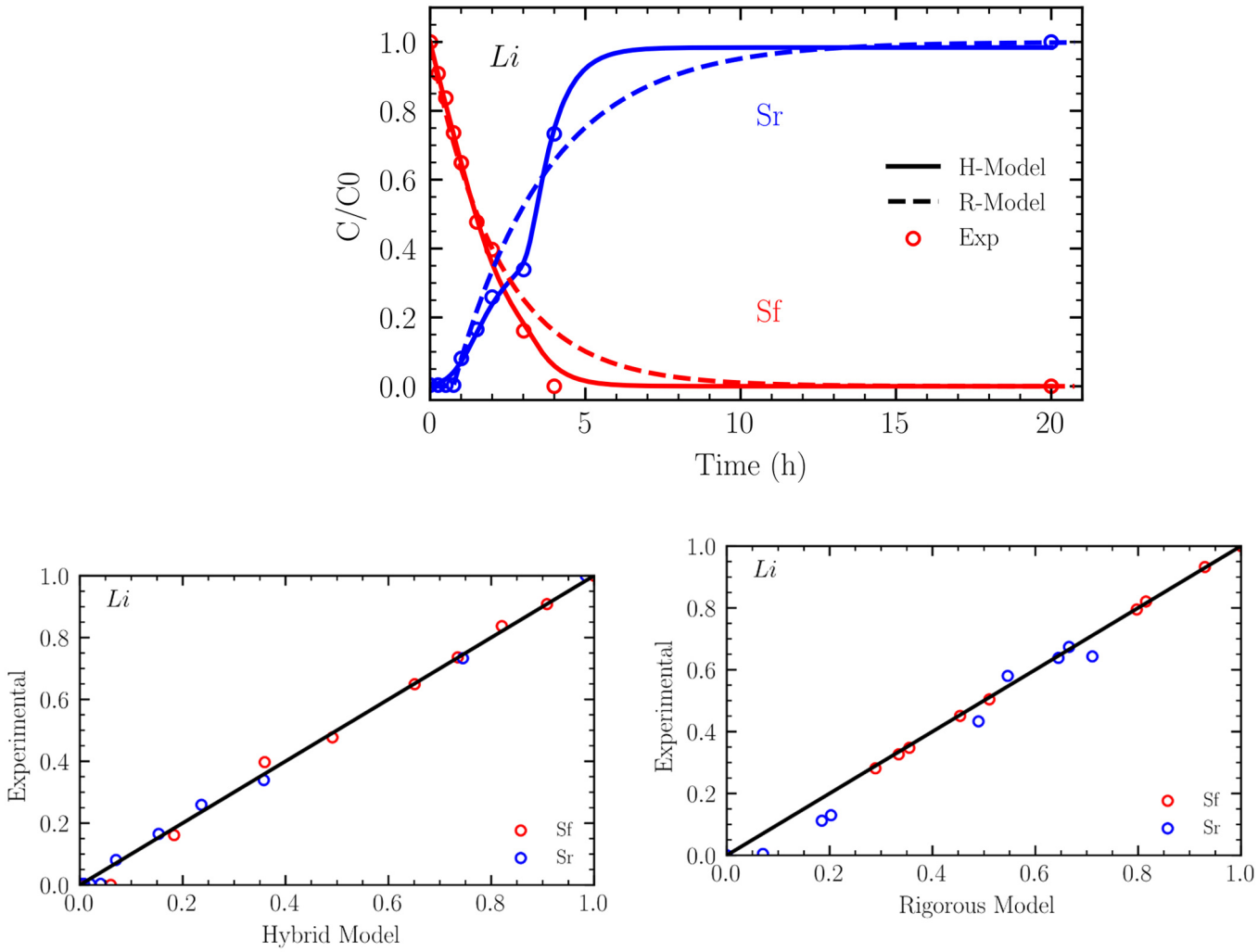

Figure 4. Lithium experimental set 1—Hybrid model prediction (H-Model) vs. the phenomenological model prediction (R-Model), and their respective parity graphics.

Another experimental set was used to demonstrate the hybrid model prediction for the lithium separation, of which results are presented in Figure 5. This experimental data were obtained from Zante et al. (2020) [24], which was conducted for a feed-phase composition of LiCl (619 mg/L) and receiving-phase composition of Na2CO3 and NaHCO3. This liquid membrane was impregnated with a mixture of hydrophobic ionic liquid 1-butyl-3-methylimidazolium bis(trifluoromethylsulfonyl)imide and tri-n-butyl phosphate as the carrier. From Figure 5, it is possible to see that the proposed hybrid model could predict the dynamic behavior of this separation with precision. In contrast, the phenomenological model presented difficulties in predicting the initial transient state.

Still, in Figure 5, it is also possible to analyze the model residuals in the parity. It can be observed that the predictions from the hybrid model are randomly distributed around the diagonal line across the whole range of values. On the other hand, the phenomenological model presents a nonrandom pattern within some regions. As before, these points correspond to the transient regime of the process, reinforcing the limitation in the phenomenological model mentioned above.

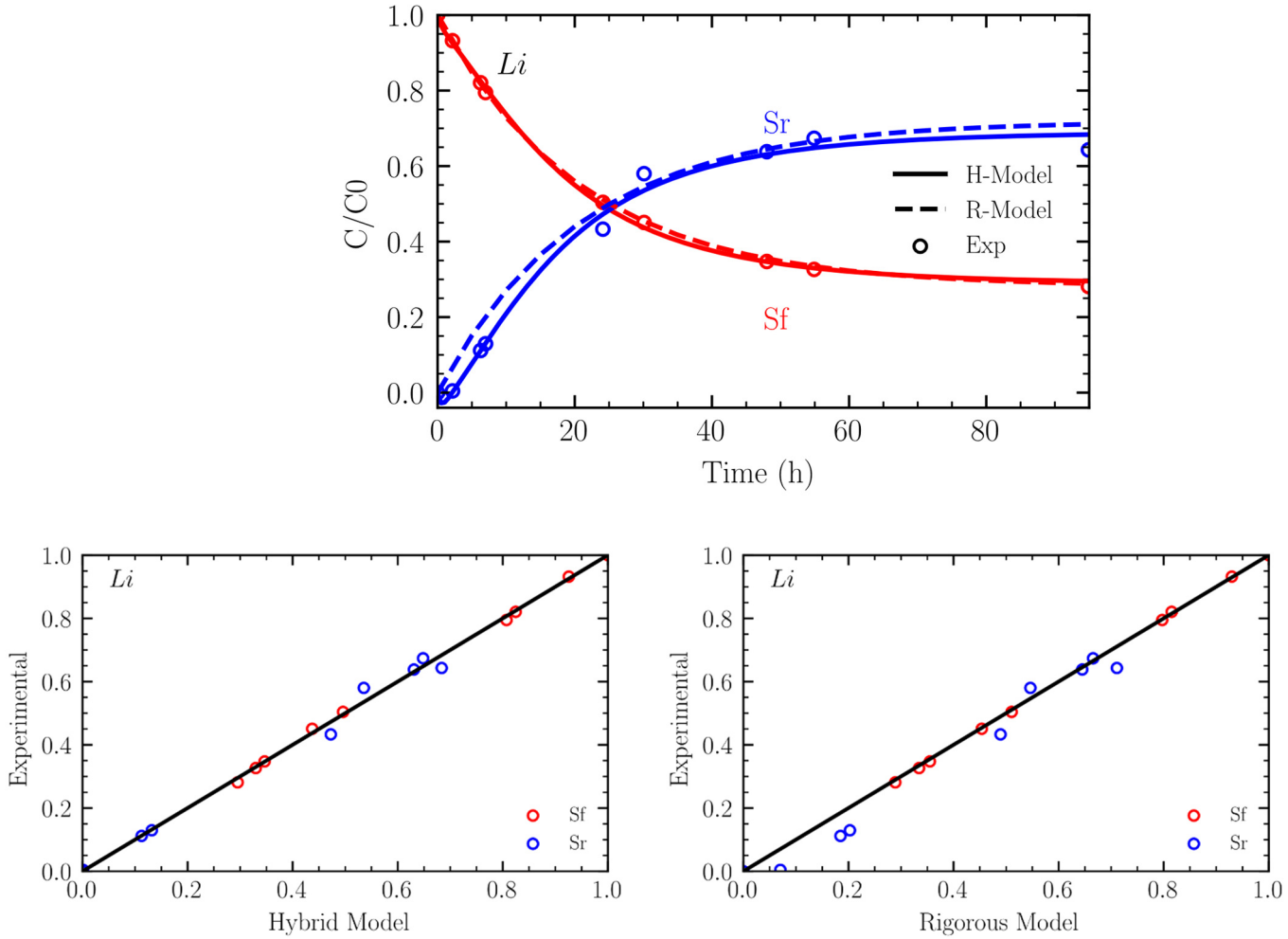

Figure 5. Lithium experimental set 2—hybrid model prediction (H-Model) vs. the phenomenological model prediction (R-Model), and their respective parity graphics.

The same hybrid modeling strategy was applied to other ions' separation. This was performed to evaluate the method's precision compared with the phenomenological approach in scenarios other than lithium recovery. The same analysis performed in the lithium recovery case can be performed with similar conclusions using this experimental validation set for different ions. Figures 6–8 present the models' predictions and the parity graphics for a series of eight experiments. The hybrid model is presented as H-model, and the phenomenological model is presented as R-model. It is essential to highlight that the experimental validation sets were another independent system obtained from the literature. As it is possible to see in Figures 6–8, the hybrid model also presents superior results and significant precision. In Figure 8, the hybrid model behavior is very similar to the phenomenological model.

The tendencies observed in the lithium case are also observed in Figures 6–8. On the one hand, the proposed hybrid model could precisely describe the systems' dynamic transition. On the other hand, the phenomenological model presented limitations predicting their dynamics. This demonstrates the potential of this synergy between phenomenological knowledge and artificial intelligence. The AI model adds more flexibility to the description of the system phenomenology, better describing the mass transfer resistance. One can analyze these results from the following perspective: while the solely phenomenological model needs to identify a parameter that can fully describe the mass transfer of the system, the AI tries to understand the mass transfer resistance and store this knowledge in a series of simple mathematical operations.

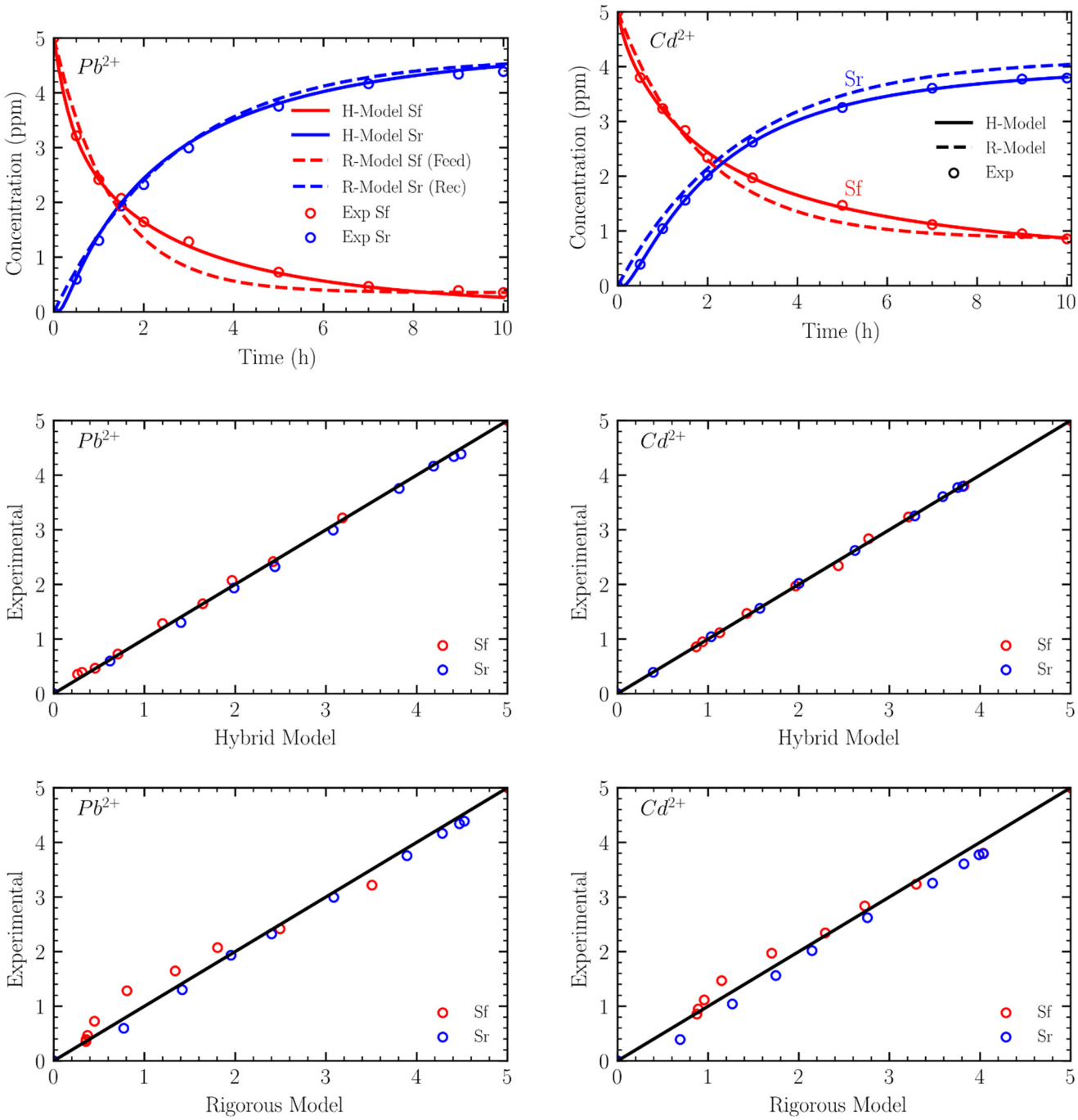

Figure 6. Experimental sets 3 and 4—hybrid model prediction vs. the phenomenological model prediction, and their respective parity graphics.

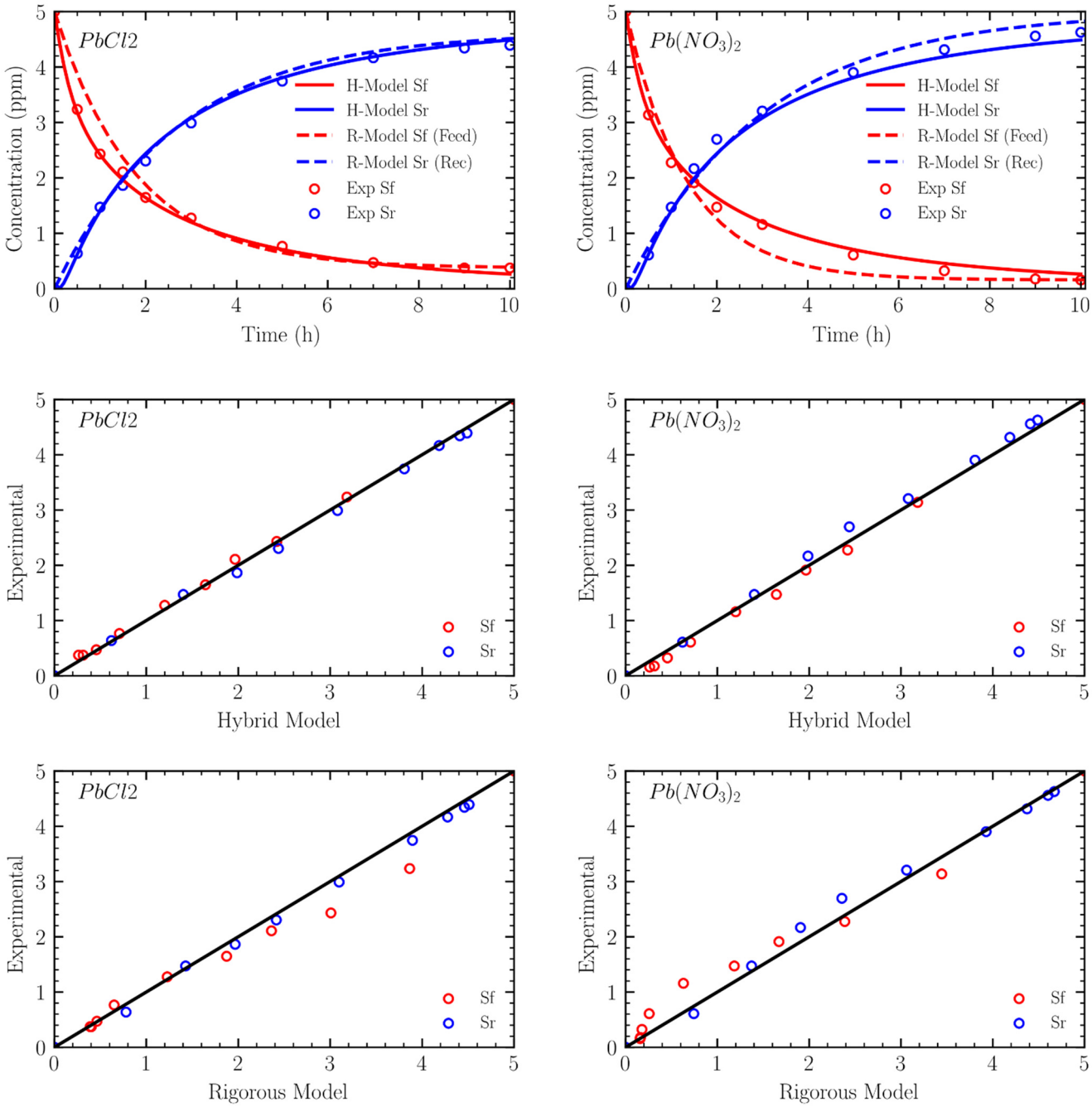

Figure 7. Experimental sets 4 and 5—hybrid model prediction vs. the phenomenological model prediction, and their respective parity graphics.

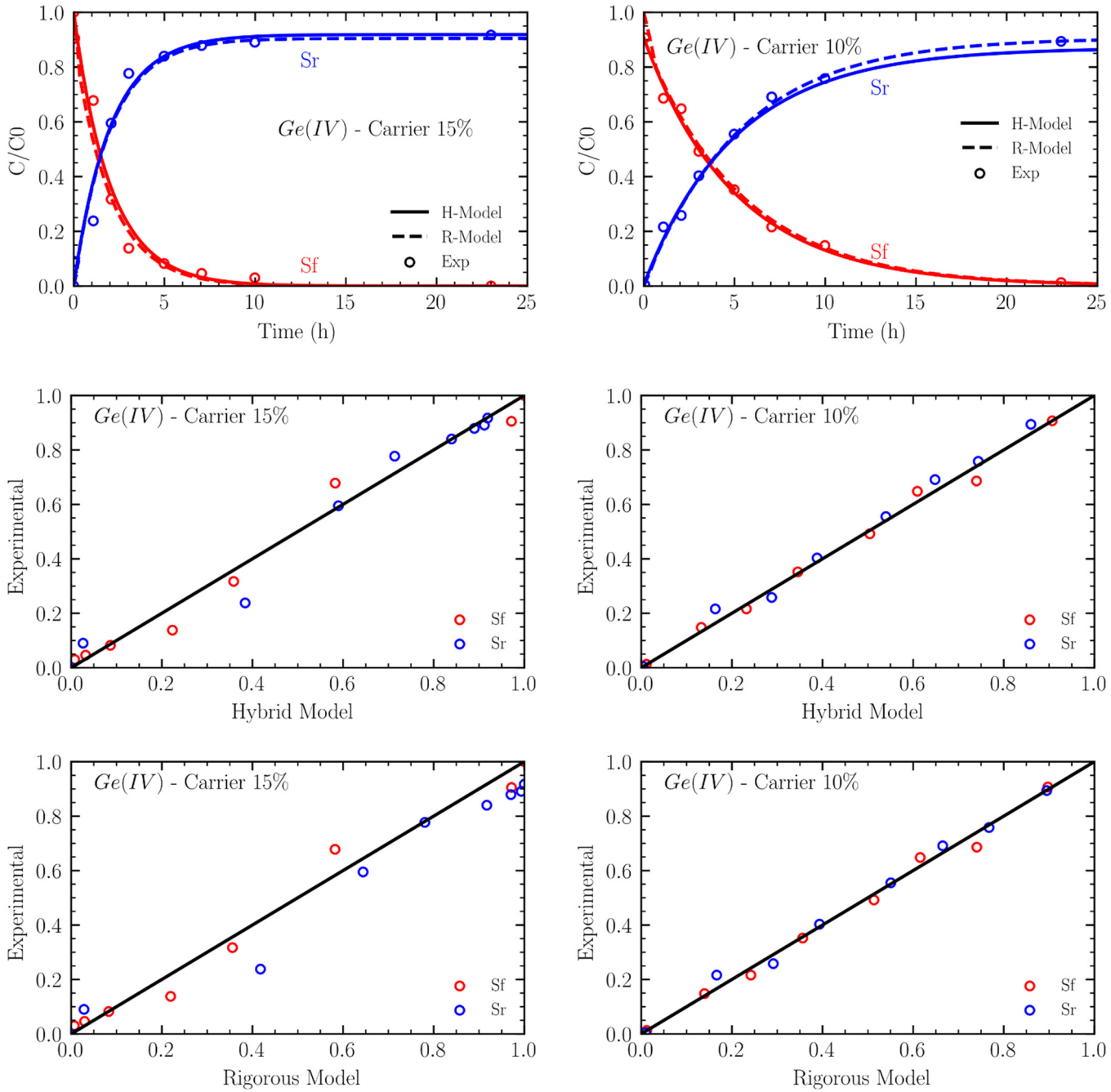

Figure 8. Experimental sets 6 and 7—hybrid model prediction vs. the phenomenological model prediction, and their respective parity graphics.

4. Conclusions

This work proposed a hybrid modeling framework to build a complete dynamic model to represent the flat-sheet supported liquid membrane (FSSLM) for lithium recovery. A phenomenological model was used to describe the system dynamic evolution. In contrast, a surrogate model was employed to represent the mass transport phenomena within the system. This approach was presented as an alternative to the traditional first-principle modeling that embeds the mass transfer phenomena into parameters that need to be identified.

The main advantage of the proposed framework is that it is possible to extract more information regarding the system and store it within an artificial neural network structure.

As the results show, this strategy yields models more precise than the phenomenological model solely.

Furthermore, the hybrid strategy can leverage the flexibility of empirical models to better understand the system in the study, for example, the system behavior in possible scenarios of mass transfer resistance. Moreover, it can potentiate the studies regarding the manipulation of the process component to harness its recovery.

Author Contributions: Conceptualization, I.B.R.N., M.J.R., V.V.S. and J.M.L.; methodology, I.B.R.N., V.V.S. and J.M.L.; software, I.B.R.N. and V.V.S.; writing—original draft preparation, I.B.R.N. and M.J.R.; writing—review and editing, I.B.R.N., A.F.P.F., J.M.L. and A.M.R.; supervision, I.B.R.N., J.M.L., A.F.P.F. and A.M.R. All authors have read and agreed to the published version of the manuscript.

Funding: This research was funding by Project "LIMEX—Innovative Membrane Extraction of Lithium for Spent Lithium-Ion Battery Recycling" funded by FCT—Fundação para a Ciência e Tecnologia through ERA-NET-European Research Area Networks Programme. This work was also financially supported by: Base Funding—UIDB/50020/2020 of the Associate Laboratory LSRE-LCM-funded by national funds through FCT/MCTES (PIDDAC) and FCT—Fundação para a Ciência e Tecnologia under the CEEC Institucional program.

Conflicts of Interest: The authors declare no conflict of interest.

References

1. Nogueira, I.B.R.; Ribeiro, A.M.; Requião, R.; Pontes, K.V.; Koivisto, H.; Rodrigues, A.E.; Loureiro, J.M. A quasi-virtual online analyser based on an artificial neural networks and offline measurements to predict purities of raffinate/extract in simulated moving bed processes. *Appl. Soft Comput. J.* **2018**, *67*, 29–47. [CrossRef]
2. Oliveira, L.M.C.; Dias, R.; Rebello, C.M.; Martins, M.A.F.; Rodrigues, A.E.; Ribeiro, A.M.; Nogueira, I.B.R. Artificial Intelligence and Cyber-Physical Systems: A Review and Perspectives for the Future in the Chemical Industry. *AI* **2021**, *2*, 429–444. [CrossRef]
3. Martins, M.A.F.; Rodrigues, A.E.; Loureiro, J.M.; Ribeiro, A.M.; Nogueira, I.B.R. Artificial Intelligence-oriented economic non-linear model predictive control applied to a pressure swing adsorption unit: Syngas purification as a case study. *Sep. Purif. Technol.* **2021**, *276*, 119333. [CrossRef]
4. Narayanan, H.; Seidler, T.; Luna, M.F.; Sokolov, M.; Morbidelli, M.; Butté, A. Hybrid Models for the simulation and prediction of chromatographic processes for protein capture. *J. Chromatogr. A* **2021**, *1650*, 462248. [CrossRef]
5. Mogk, G.; Mrziglod, T.; Schuppert, A. Application of Hybrid Models in Chemical Industry. In *Computer Aided Chemical Engineering*; Elsevier: Amsterdam, The Netherlands, 2002; Volume 10, pp. 931–936. [CrossRef]
6. Narayanan, H.; Luna, M.; Sokolov, M.; Arosio, P.; Butté, A.; Morbidelli, M. Hybrid Models Based on Machine Learning and an Increasing Degree of Process Knowledge: Application to Capture Chromatographic Step. *Ind. Eng. Chem. Res.* **2021**. [CrossRef]
7. Nagrath, D.; Messac, A.; Bequette, B.W.; Cramer, S.M. A Hybrid Model Framework for the Optimization of Preparative Chromatographic Processes. *Biotechnol. Prog.* **2004**, *20*, 162–178. [CrossRef] [PubMed]
8. Benzal, G.; Kumar, A.; Delshams, A.; Sastre, A.M. Mathematical modelling and simulation of cotransport phenomena through flat sheet-supported liquid membranes. *Hydrometallurgy* **2004**, *74*, 117–130. [CrossRef]
9. León, G.; Martínez, G.; León, L.; Guzmán, M.A. Separation of cobalt from nickel using novel ultrasound-prepared supported liquid membranes containing Cyanex 272 as carrier. *Physicochem. Probl. Miner. Process.* **2016**, *52*, 77–86. [CrossRef]
10. Wang, D.; Chen, Q.; Hu, J.; Fu, M.; Luo, Y. High Flux Recovery of Copper(II) from Ammoniacal Solution with Stable Sandwich Supported Liquid Membrane. *Ind. Eng. Chem. Res.* **2015**, *54*, 4823–4831. [CrossRef]
11. Peydayesh, M.; Esfandyari, G.R.; Mohammadi, T.; Alamdari, E.K. Pertraction of cadmium and zinc ions using a supported liquid membrane impregnated with different carriers. *Chem. Pap.* **2013**, *67*, 389–397. [CrossRef]
12. Lantto, J. *Analytical Model of Mass Transfer through Supported Liquid Membranes*; Kungliga Tekniska Hogskolan: Stockholm, Sweden, 2015.
13. Regufe, M.J.; Ribeiro, A.M.; Ferreira, A.F.P.; Loureiro, J.M. Complete and simplified modelling of flat sheet supported liquid membranes for the extraction of metal ions. *Intern. Rep. Porto.* **2021**, *21*, 1–20.
14. Ofori-Sarpong, G.; Amankwah, R.K. Comminution environment and gold particle morphology: Effects on gravity concentration. *Miner. Eng.* **2011**, *24*, 590–592. [CrossRef]
15. Sun, Y.; Wang, Q.; Wang, Y.; Yun, R.; Xiang, X. Recent advances in magnesium/lithium separation and lithium extraction technologies from salt lake brine. *Sep. Purif. Technol.* **2021**, *256*, 117807. [CrossRef]
16. Zheng, J.; Kim, M.S.; Tu, Z.; Choudhury, S.; Tang, T.; Archer, L.A. Regulating electrodeposition morphology of lithium: Towards commercially relevant secondary Li metal batteries. *Chem. Soc. Rev.* **2020**, *49*, 2701–2750. [CrossRef]
17. Maxwell, P. Analysing the lithium industry: Demand, supply, and emerging developments. *Miner. Econ.* **2014**, *26*, 97–106. [CrossRef]

18. Gerold, E.; Luidold, S.; Antrekowitsch, H. Separation and Efficient Recovery of Lithium from Spent Lithium-Ion Batteries. *Metals* **2021**, *11*, 1091. [CrossRef]
19. Azevedo, M.; Campagnol, N.; Hagenbruch, T.; Hoffman, K.; Lala, A.; Ramsbottom, O. Lithium and Cobalt: A Tale of Two Commodities. Available online: https://www.mckinsey.com/industries/metals-and-mining/our-insights/lithium-and-cobalt-a-tale-of-two-commodities (accessed on 15 May 2021).
20. Zheng, J.; Archer, L.A. Controlling electrochemical growth of metallic zinc electrodes: Toward affordable rechargeable energy storage systems. *Sci. Adv.* **2021**, *7*, 1–20. [CrossRef] [PubMed]
21. Patil, N.; Sharma, A.; Patwardhan, A. Process Intensification Using Hollow Fibre-supported Liquid Membranes. *Indian Chem. Eng.* **2015**, *57*, 1–22. [CrossRef]
22. Bhatluri, K.K.; Manna, M.S.; Ghoshal, A.K.; Saha, P. Supported liquid membrane based removal of lead(II) and cadmium(II) from mixed feed: Conversion to solid waste by precipitation. *J. Hazard. Mater.* **2015**, *299*, 504–512. [CrossRef]
23. Zaheri, P.; Ghassabzadeh, H.; Abolghasemi, H.; Maraghe, M.G.; Mohammadi, T. Facilitated transport of Europium through supported liquid membrane using Cyanex272 as carrier and mass transfer modelling. *Can. J. Chem. Eng.* **2017**, *95*, 524–534. [CrossRef]
24. Zante, G.; Boltoeva, M.; Masmoudi, A.; Barillon, R.; Trébouet, D. Highly selective transport of lithium across a supported liquid membrane. *J. Fluor. Chem.* **2020**, *236*, 109593. [CrossRef]
25. Zante, G.; Boltoeva, M.; Masmoudi, A.; Barillon, R.; Trébouet, D. Lithium extraction from complex aqueous solutions using supported ionic liquid membranes. *J. Memb. Sci.* **2019**, *580*, 62–76. [CrossRef]
26. Zante, G.; Boltoeva, M.; Masmoudi, A.; Barillon, R.; Trébouet, D. Selective separation of cobalt and nickel using a stable supported ionic liquid membrane. *Sep. Purif. Technol.* **2020**, *252*, 117477. [CrossRef]
27. Rebello, C.M.; Martins, M.A.F.; Loureiro, J.M.; Rodrigues, A.E.; Ribeiro, A.M.; Nogueira, I.B.R. From an Optimal Point to an Optimal Region: A Novel Methodology for Optimization of Multimodal Constrained Problems and a Novel Constrained Sliding Particle Swarm Optimization Strategy. *Mathematics* **2021**, *9*, 1808. [CrossRef]